ARTICLE IN PRESS

THE JOURNAL OF PROSTHETIC DENTISTRY

RESEARCH AND EDUCATION

Dental biomechanics of root-analog implants in different bone types

João Paulo M. Tribst, DDS, PhD,[a] Amanda Maria de O. Dal Piva, DDS, PhD,[b] Erik J. Blom, DDS,[c] Cornelis J. Kleverlaan, DDS, PhD,[d] and Albert J. Feilzer, DDS, PhD[e]

ABSTRACT

Statement of problem. When implants are applied to restore oral function, the masticatory load on the crown will lead to stress development in all parts of the crown-abutment-implant-bone system. An optimal design of the whole system will be important for sustained function.

Purpose. The purpose of this 3-dimensional (3D) finite element analysis (FEA) study was to evaluate the influence of the root-analog implant (RAI) design in molar rehabilitation and bone type.

Material and methods. Twelve 3D models of single posterior implant-supported restorations were created according to the zirconia implant design (monotype, 2-piece, or RAI) and bone type (D1, D2, D3, and D4, according to the Misch classification). The models were composed of cortical bone, cancellous bone, implant, cement layers, and a monolithic ceramic crown. For the 2-piece zirconia implant model, the titanium base, prosthetic screw, and framework were also designed. All materials were assumed to behave elastically throughout the entire analysis. The bone was fixed, and an axial loading of 600 N was applied to the contacts on the occlusal surface of the crowns. Results for the crown and implant were obtained in maximum principal stress, as well as the von Mises stress for the model and bone microstrain.

Results. High stress concentration was observed at the intaglio surface of the crowns near the loading region. Regardless of the design, the stress trend in the implant was similar, increasing proportionally to the bone type (D1>D2>D3>D4). RAI showed a homogeneous stress field near the values calculated for the conventional designs, but with lower magnitudes. The 2-piece zirconia model showed the highest stress magnitude regardless of the bone type and, therefore, the highest failure risk. All models showed a higher strain in the cortical bone than in the cancellous bone, located predominantly in the cervical region. A strain analysis showed that both conventional implant models presented similar behavior for D1 and D2 bone types, with an increasing difference for D3 and D4. RAI showed the lowest strain regardless of the bone type.

Conclusions. Root-analog zirconia implants present a promising biomechanical behavior for dissipating the masticatory load in comparison with conventional screw-shaped implants. (J Prosthet Dent 2022;■:■-■)

During evolution, tooth morphology developed to process food with minimal energy and ensure that induced stresses are optimally absorbed by the teeth, periodontal ligament, and bone.[1-7] Implant-supported restorations have been used extensively to replace lost teeth,[3-10] with long-term success rates reported to be between 90% and 100% after 10-year follow-up.[4] However, the prevalence of peri-implant mucositis has reported to range from 19% to 65% and peri-implantitis from 1% to 47%.[5] Peri-implantitis is an inflammation associated with severe bone loss that leads to implant loss.[6,11-14] Three of 5 patients with implant-supported maxillary overdentures have been reported to experience peri-implant mucositis, and peri-implantitis

[a]Assistant Professor, Department of Oral Regenerative Medicine, Academic Centre for Dentistry Amsterdam (ACTA), Universiteit van Amsterdam and Vrije Universiteit, Amsterdam, the Netherlands.
[b]Assistant Professor, Department of Dental Materials Science, Academic Centre for Dentistry Amsterdam (ACTA), Universiteit van Amsterdam and Vrije Universiteit, Amsterdam, the Netherlands.
[c]Associate Professor, Department of Oral Regenerative Medicine, Academic Centre for Dentistry Amsterdam (ACTA), Universiteit van Amsterdam and Vrije Universiteit, Amsterdam, the Netherlands.
[d]Professor, Department of Dental Materials Science, Academic Center for Dentistry Amsterdam (ACTA), University of Amsterdam & Vrije Universiteit, Amsterdam, the Netherlands.
[e]Professor, Department of Oral Regenerative Medicine, Academic Center for Dentistry Amsterdam (ACTA), University of Amsterdam & Vrije Universiteit, Amsterdam, the Netherlands.

Clinical Implications

The suitable stress distribution of zirconia root-analog implants, in all bone types, suggests that this implant option might be appropriate for the replacement of molars.

occurred in 1 of 5 patients after 10 years [15] Therefore, complications are to be expected when considering peri-implant tissue stability. After 18 years, the type of prosthesis was identified as a risk factor for the development of a peri-implant disease, as well as a history of peri-implantitis and unfavorable load distribution.[16] In addition, implant-retained removable prostheses were associated with more bone loss than other implant-supported prostheses.[16]

Because of the popularity of dental implants, even a low incidence of peri-implantitis would greatly affect oral care budgets.[6] While the peri-implantitis etiology is still not clear, the lack of a periodontal ligament and the shape of the implant suggest that stress formation at the implant-bone interface may play a role.[3-6] Mechanical stress loaded to bone is associated with remodeling and might result in bone loss around the implant with overload.[7,17,18] Whether contemporary implant designs are well designed from a biomechanical perspective is unclear,[18-28] particularly as the screw type cylinder is more wedge-shaped than a natural tooth root.

The surface of the implant,[28] its macrogeometry,[6] prosthetic connection,[7] taper,[8] thread design,[9] loading direction,[10] bone connection,[11] and type[23] can modify primary and secondary stability. Implant design has been optimized in terms of biocompatibility, strength, and surgical handling.[3,13,24-26] Therefore, different designs emerged, including Scialom needles,[24] Garbaccio bicortical implants,[25] and Pasqualini universal biphasic blades,[26] until the screw-shaped design popularized by the Brånemark protocol was adopted.[13] Nevertheless, implants were standardized with a prefabricated design and not as a patient-specific appliance.[19] Therefore, primary stability in recent extraction sockets can be achieved by placing an implant larger than the alveolar apex or by using an implant of greater diameter than the socket walls.[20] Based on the tooth model, root-shaped or root-analog implants (RAIs) emerged as a treatment alternative to traditional threaded implants.[20,21,29,30] RAIs were first described in 1969 and manufactured with polymethacrylate and without osseointegration.[31] In 1992, the concept was reintroduced in titanium alloy and with the claim that intact sockets offered an optimal environment for implantation.[31] However, information regarding the dissipation of masticatory forces with RAIs is scarce and controversial. Therefore, how the implant design could modify the load dissipation through the bone is unclear, justifying the present study that helps develop an implant design with optimal load distribution.

Implant placement should be dependent on a biomechanical algorithm customized for each patient.[32] Understanding how mechanical stresses and strain influence peri-implant bone loss may suggest that the tooth model provides a suitable guide for implant design and may help explain the prevalence of peri-implantitis.[14] To investigate how restorations function, different methodologies have been applied in an attempt to replicate the complex conditions of the oral cavity.[6,10,13,21,22,33] Finite element analysis (FEA) uses a mathematical analysis to model restorative systems by differentiating their mechanical properties and subjecting them to different evaluation conditions.[10,22,27,33] FEA has been widely used in dentistry to analyze mechanical behaviors as an indicator of areas where stresses are concentrated, potential areas of clinical fracture, or areas that can influence bone remodeling. Knowledge from FEA allows the clinical selection of more favorable procedures with improved clinical success.[10,11,14,22]

This study aimed to analyze the stress distributions around zirconia implants by comparing a custom-designed RAI with a natural root shape versus a monotype and a 2-piece conventional implant considering different bone types. The research hypothesis was that the biomechanical behavior, that is, low stress at the implant-bone interface, would be optimal with the RAI.

MATERIAL AND METHODS

Three-dimensional (3D) FEA was used to investigate the biomechanical behavior of different zirconia implants. The evaluated condition using root-analog implants was adapted from the workflow described by Liu et al[21] after the surgery stage (Fig. 1). The major steps to obtain custom dental implants were considered in the second stage of bone maturation, after the healing period, and with complete osseointegration. The solid bone tissue was modeled based on a 3D structure of a sectioned jaw, containing cortical (1.0-mm-thick) and cancellous bone tissues[22] (Fig. 2). Different zirconia implant designs for replacing a missing molar were created by using a computer-aided design (CAD) software program (Rhinoceros 5.0; McNeel Europe): 2-piece implant (4.1×10-mm implant, Pure Ceramic Implant; Institut Straumann AG) and zirconia abutment (4.0 mm, PUREbase Abutment; Institut Straumann AG); monotype implant (4.1×10-mm implant and 4.0-mm abutment height; PURE Ceramic Implant Monotype; Institut Straumann AG); and RAI (10 mm in height) (Fig. 3). The monotype and 2-piece models were exported to the CAD software program and positioned in the center of the cortical bone tissue similar to the bone-level implant concept.[22] The RAI model was created based on a human tooth

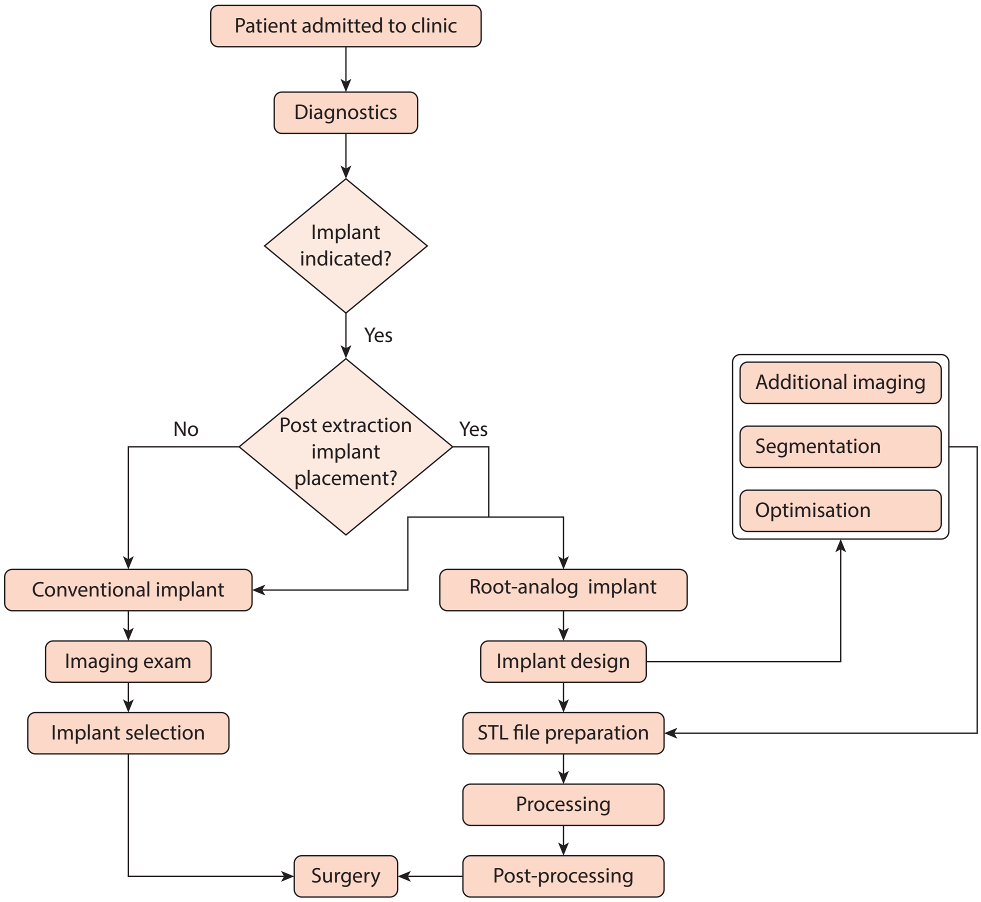

Figure 1. Workflow for patient-specific implants in dental applications adapted from workflow described by Liu et al.[21] STL, standard tessellation language.

prepared for a complete crown.[33] The bone model was replicated to receive 1 of the implant designs. A monolithic crown was cemented over the implants with a similar external anatomy and occlusal shape, with the intaglio surface adapted according to the adhesive area of the abutment. All crown models had a minimal thickness of 1.5 mm at the center of the crown and a layer of 0.1-mm-thick resin cement (Fig. 3).

The geometries were imported into a computer-aided engineering software program (ANSYS 17.2; ANSYS Inc) as STandard for the Exchange of Product model data (STEP) files. The parametric subdivision was created after the mesh convergence test. Tetrahedral elements with 10% degrees of freedom for convergent values were applied. The mesh size was based on the maximum von Mises stress values located at the cervical bone level. The mesh density parameters were finally standardized with element quality defined as 0.81 ±0.92, an aspect ratio of 1.80 ±0.87, an average maximum corner angle of 87.44 degrees, and a skewness average of 0.19 ±0.11. The inflation option of smooth transition was applied between the solids, and the rigid body behavior was standardized as dimensionally reduced. After the meshing process, the total number of elements and nodes for monotype (406 838 and 250 129), 2-piece (429 416 and 238 191), and RAI (357 403 and 188 726) models were defined. As boundary conditions, the load was defined as a vector in the direction of the Z-axis with 600-N magnitude (Fig. 4). All materials were assumed to be isotropic and linear and to have an elastic behavior and a homogeneous structure. The contact between the implant and bone was simulated with complete osseointegration, and all connections were considered to have bonded contact. The external surface of the bone model was fixed in all directions.

The static structure analysis was performed for the function of 2 constants: elastic modulus and Poisson ratio. The required data for the assessment were then determined from the literature and summarized in Table 1.[22,27,32-34] The results of stress magnitude were calculated according to the von Mises criteria (MPa) for sectioned models. The maximum principal stress criteria were used to investigate the tensile stress distribution in brittle materials (zirconia implants and lithium disilicate crowns). The microstrain (με) criteria were used to investigate the behavior of the cortical and cancellous

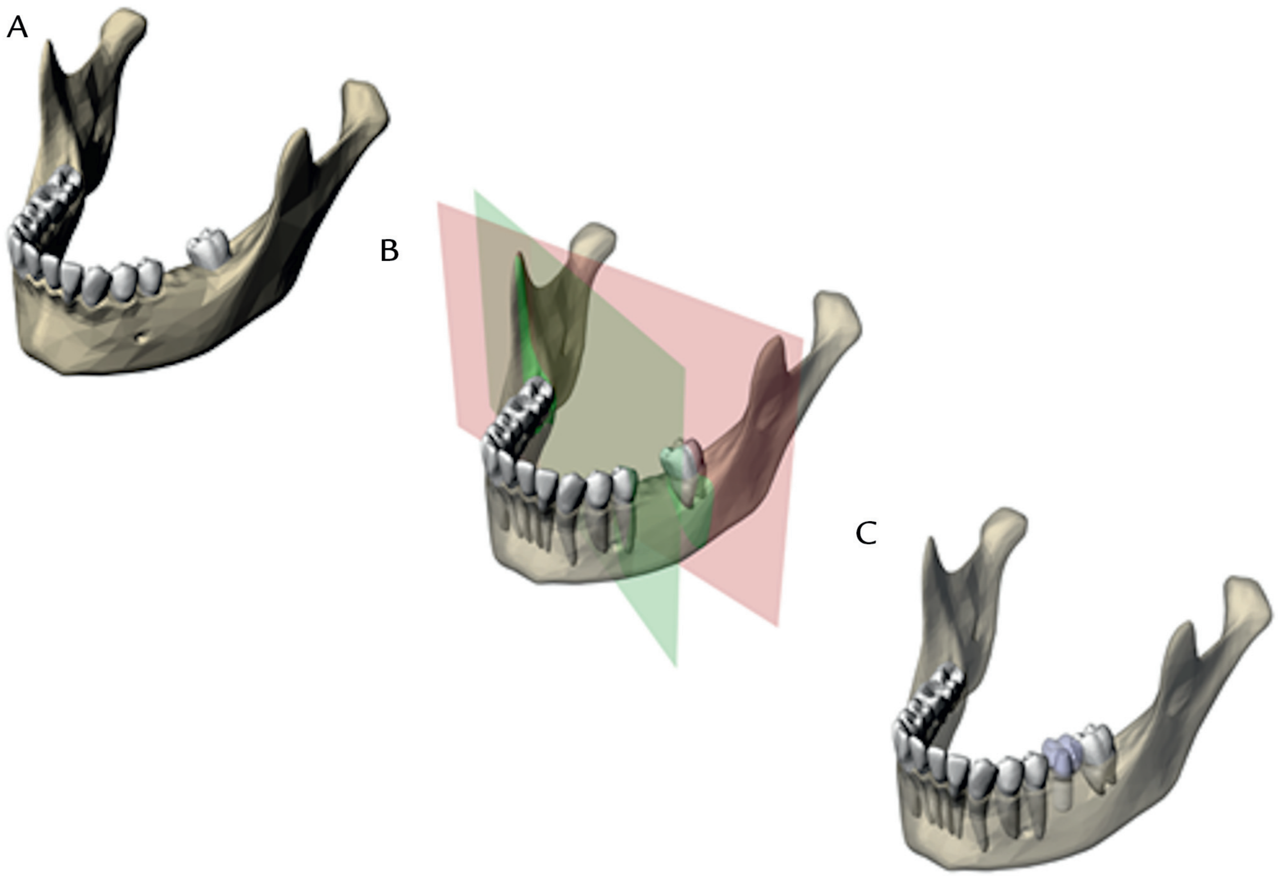

Figure 2. Modeling of jaw volumetric structure with missing molar. A, Edentulous space. B, Cross-section for bone tissue standardization. C, Implant positioning.

bone tissues. The maximum microstrain values are shown in Table 2. Bone type identification followed the classification described by Misch[18] according to the bone density: dense cortical bone (D1), porous cortical and coarse cancellous bone (D2), porous cortical bone (thin) and fine cancellous bone (D3), and fine cancellous bone (D4). To evidence the effect of the implant design, the bone strain was calculated based on the Wolff Law and bone's structural adaptation to mechanical usage.[17]

RESULTS

According to von Mises stress (Fig. 5), the RAI design presented the best stress distribution. A high stress concentration was observed in a similar trend at the crown intaglio surface near the loading site at the center of the models. The fulcrum region of the cervical level of the cortical bone tissue was also observed. Despite the similarities, the stress magnitude in the other regions was visible and differed between distinct implant designs and bone types.

The stress distribution in the restoration was not visibly affected by the bone type or implant design (Fig. 6). Isolating the crown intaglio surface, the tensile stress area was located near the loading application point and coincident to the thinnest area of the ceramic. RAI showed a lower stress concentration at the restoration margin. However, for all designs, the highest stress concentration was coincident with failures starting at the adhesive interface. In addition, higher stress levels were observed near the restoration margin for monotype and 2-piece models but with a lower magnitude than at the center of the crown.

Regardless of the implant, the stress trend was similar among the models (Fig. 7), increasing proportionally to the bone type classification (D1>D2>D3>D4). The 2-piece design showed the highest stress concentration region, caused by the fulcrum at the abutment joint. RAI showed a homogeneous and comparable stress field near the stress values calculated for the other designs. However, it showed a new stress concentration area at the separation of the roots contacting the bone septum instead of only at the lateral region as in the other models. This effect was more evident for bone types D3 and D4 when the stress level magnitude increased.

The autoprobe tool from the Mechanical ANSYS Parametric Design Language (APDL) selected the region of highest stress magnitude, and stress peaks are summarized in Table 2. For a similar bone, the RAI showed

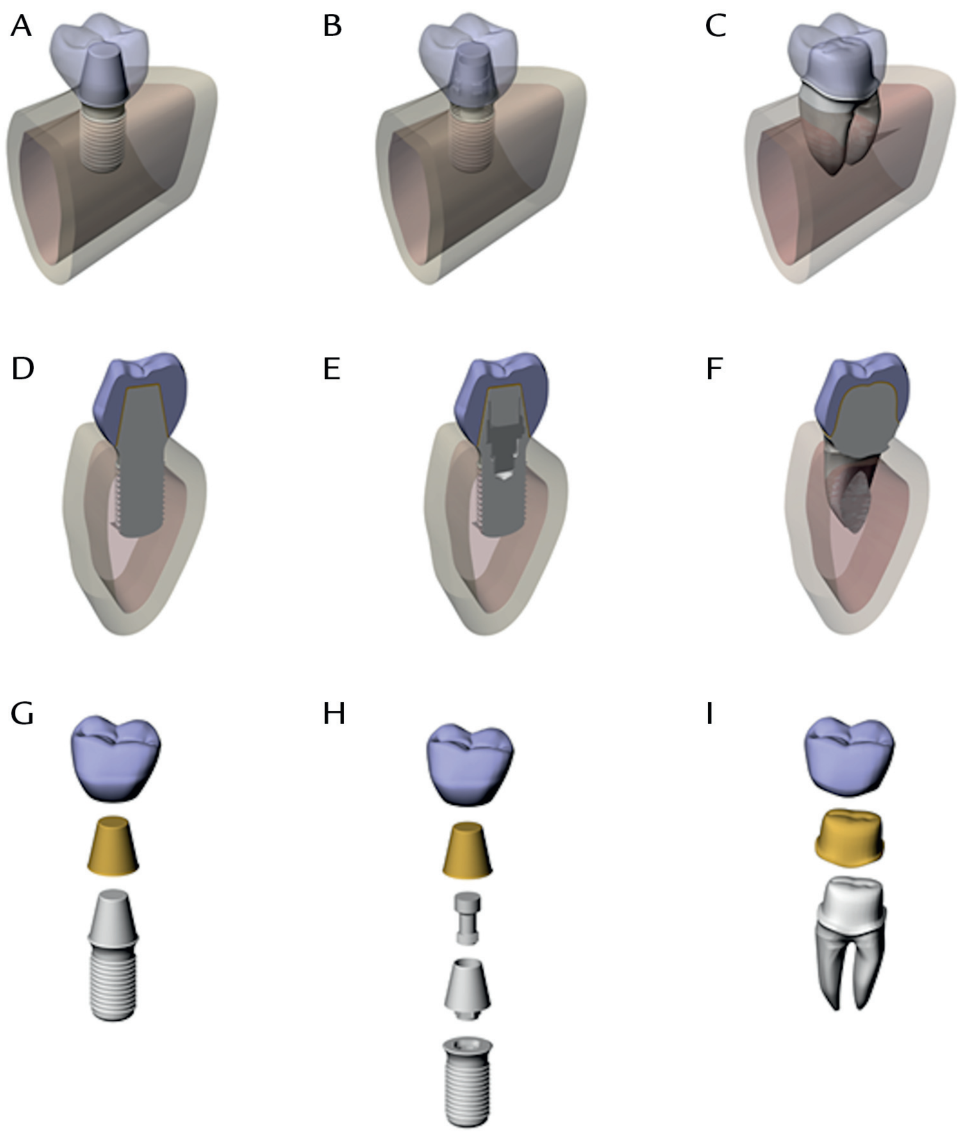

Figure 3. Modeling of implant designs according to different conditions. Isometric view: A, monotype zirconia implant; B, 2-piece zirconia implant; C, root-analog zirconia implant. Section-plane view: D, monotype zirconia implant; E, 2-piece zirconia implant; F, root-analog zirconia implant. Exploded view of juxtaposed structures: G, monotype zirconia implant; H, 2-piece zirconia implant; I, root-analog zirconia implant.

the lowest stress magnitude. The 2-piece design showed the highest stress magnitude, regardless of the bone type, and, therefore, the highest failure risk in comparison to the monotype or root-analog designs. For the bone tissue mechanical response, all models showed a higher strain in the cortical bone than in the cancellous bone, located predominantly at the cervical level. Figure 8 displayed the 2D view of microstrain contour lines, showing a less-promising behavior for D4 bone tissue, regardless of the implant. Strain results (Fig. 9) showed that both the conventional models presented a similar behavior for D1 and D2 bone tissues, with increasing difference as the bone tissue became more flexible. RAIs showed the lowest strain regardless of the bone; the strain in D3 and D4 trabecular bone was similar to the strain in D1 and D2 when a conventional implant was used. The peak cortical strain, however, was below that of the nonanatomic models, suggesting the absence of lamellar bone modeling. Values of unwanted alveolar resorption were not calculated for all simulated conditions.

DISCUSSION

This study evaluated the effect of implant design and the type of bone contacting implant surfaces on stress formation. From the biomechanical point of view, using a root-analog design to replace a missing molar properly dissipated the masticatory load. Therefore, the study's hypothesis was accepted.

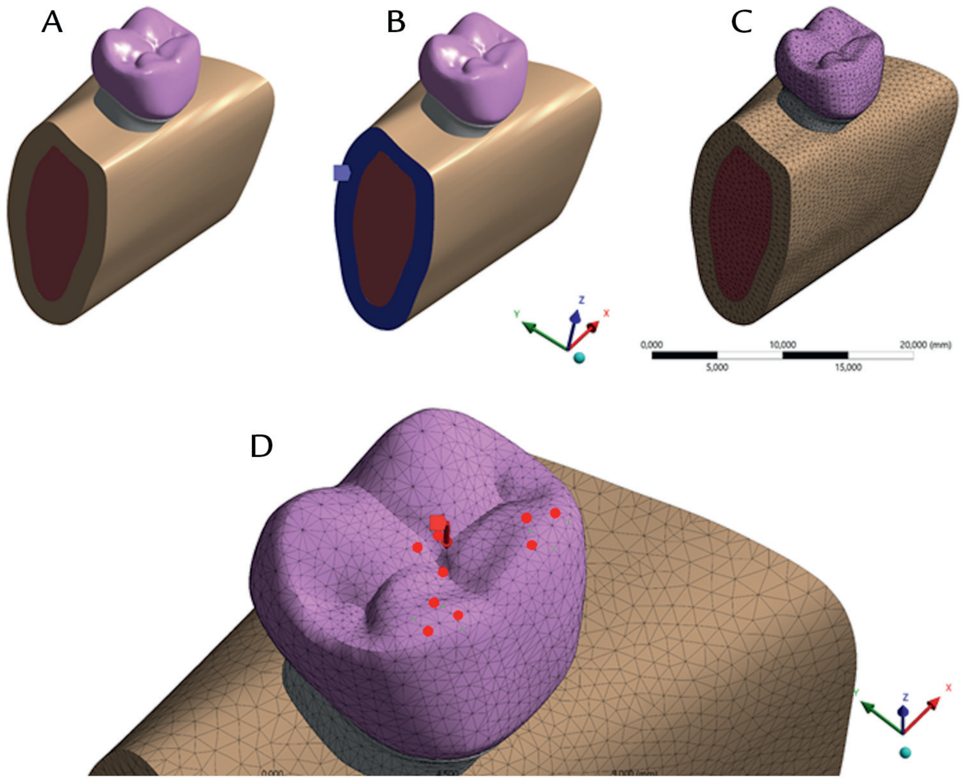

Figure 4. A, Model exported to computer-aided engineering software program. B, Fixation support defined at lateral sides of bone tissue. C, Mesh division after refinement. D, Loading condition applied at occlusal contact points in Z-axis direction.

Table 1. Mechanical properties of materials and structures simulated

Material/Structure	Elastic Modulus (GPa)	Poisson Ratio (v)
Titanium[13]	110	0.3
Zirconia[11]	200	0.3
Lithium disilicate[14]	82.3	0.22
Resin cement[12]	7	0.28
Cortical bone D1[15]	13	0.3
Cortical bone D2[15]	13	0.3
Cortical bone D3[15]	13	0.3
Cortical bone D4[15]	13	0.3
Trabecular bone D1[15]	9.5	0.3
Trabecular bone D2[15]	5.5	0.3
Trabecular bone D3[15]	1.6	0.3
Trabecular bone D4[15]	0.69	0.3

Table 2. Stress peaks in implant fixture and in crown according to implant design and bone type

Implant Design	Bone Type	Stress in Implant Fixture (MPa)	Stress in Crown (MPa)
Monotype	D1	4.52	65.42
	D2	12.83	65.41
	D3	40.33	65.39
	D4	57.20	65.20
2-Piece	D1	8.57	64.89
	D2	18.14	64.90
	D3	49.54	65.29
	D4	62.88	65.28
Root-analog	D1	3.80	64.70
	D2	10.71	64.65
	D3	34.83	64.59
	D4	49.34	64.58

Because of the development of digital dentistry with computer-aided design and computer-aided manufacturing and improved medical imaging, the root-analog design can be used to address specific needs.[35] Although RAIs require a more complex workflow, they can be successfully used to reduce the discrepancy between the synthetic implanted root and the individual tooth-extraction socket.[36,37] However, the mechanical impact of this treatment option has not previously been investigated. The present results suggest a similar mechanical behavior for the crown but a better prognosis for implant and bone. Because osseointegration is the healing mode when an RAI is inserted in the tooth socket after immediate extraction, direct contact between the bone and RAI[31] was simulated in the present study.

Most studies have used titanium alloy for root-analog implants.[9,10,29,37] Although considered as a nonallergenic material, allergic reactions to titanium have been reported.[38,39] In addition, expectations regarding esthetics are growing, making the use of zirconia dental implants a

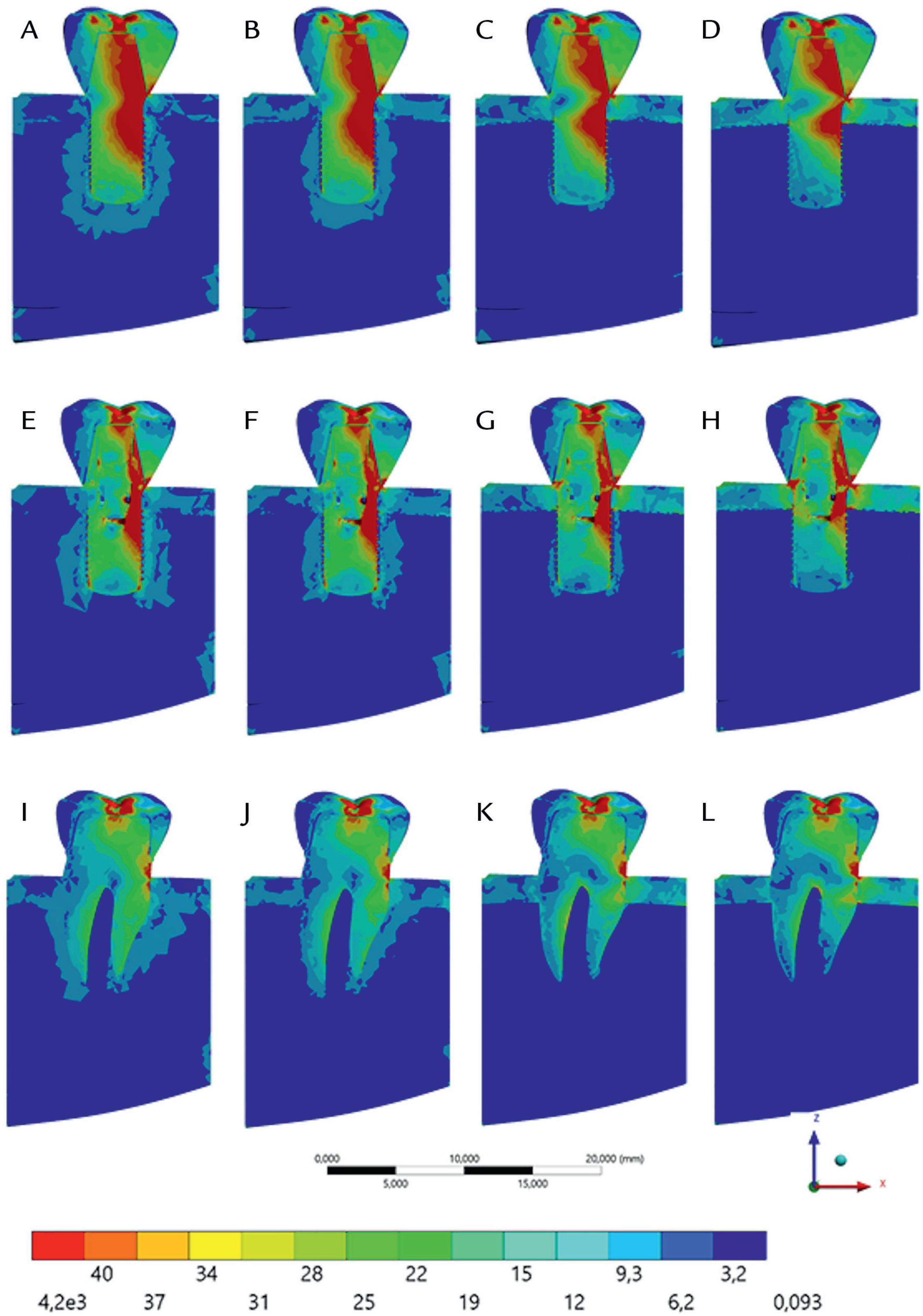

Figure 5. von Mises stress distribution according to different implant designs and bone type. Monotype implant design and bone: A, D1; B, D2; C, D3; D, D4. Two-piece design and bone: E, D1; F, D2; G, D3; and H, D4. RAI and bone: I, D1; J, D2; K, D3; L, D4.

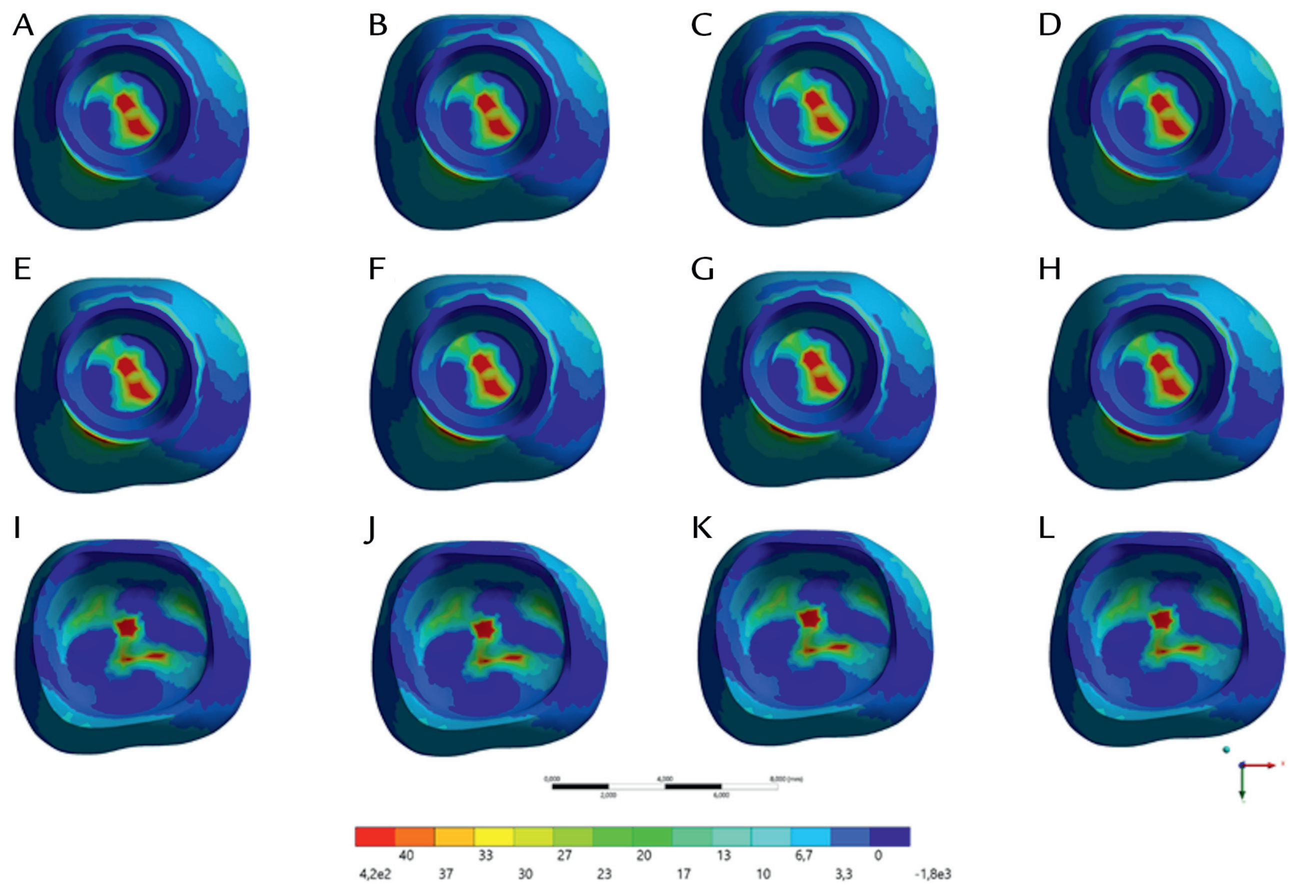

Figure 6. Maximum principal stress (tensile) distribution in crown intaglio surface according to different implant designs and bone type. Monotype implant design and bone: A, D1; B, D2; C, D3; D, D4. Two-piece design and bone: E, D1; F, D2; G, D3; H, D4. RAI and bone: I, D1; J, D2; K, D3; L, D4.

promising alternative[11] with favorable mechanical, biological, and esthetic properties.[8] The most common designs for zirconia implants are monotype or 2-piece, with a shape similar to that of conventional titanium implants with threads.[11] The treatment using a zirconia RAI immediately after tooth extraction has been reported as minimally invasive, respecting the underlying anatomy, saving time and cost, and resulting in improved esthetics leading to increased acceptance among patients.[8] However, this technique is restricted to the atraumatic extraction of a periodontally sound tooth with adequately deep sockets, sufficient bone support, and no periapical pathology.[8] This condition was simulated in the present study.

RAIs showed the lowest stress level between the evaluated implants, probably because it has a higher volume and contact area (163.15 mm^2) to dissipate the masticatory load than the other implants (48.08 mm^2). The difference between 2-piece and 1-piece implants was that the fulcrum and titanium base were acting as a more flexible joint than the solid structure. This behavior corroborates data from a previous FEA study[11] comparing 1-piece and 2-piece zirconia implants. A literature review on RAIs reported that studies with FEA showed that zirconia implants produced higher stress values on trabecular bone, protecting the cortical bone.[40] The authors reported that RAIs had high strain in cancellous bone and reduced values in cortical bone compared with the other implants. A 2-year follow-up of RAI implantation reported an unchanged peri-implant marginal bone level and soft-tissue parameters without bleeding on probing.[40] In addition, the authors stated that the single-stage implant approach led to early functional loading, allowing osseointegration while preventing alveolar resorption.[8] A 10-year follow-up clinical report of the first posterior RAI manufactured with a Ti-6Al-4V alloy and implanted in humans reported that the RAI maintained dimensional stability of the peri-implant soft tissues without crestal resorption.[9] The authors attributed the favorable outcome to the perfect match of the implant structure with the walls of the socket, the correct patient selection, a good surgical protocol, and the less-invasive implant insertion technique.[9] The present study complements these findings because the reported factors seem to be associated with osseointegration in the early stage; however, to keep the bone height stable, optimal distribution of the masticatory load should be achieved. Therefore, another factor of clinical success is

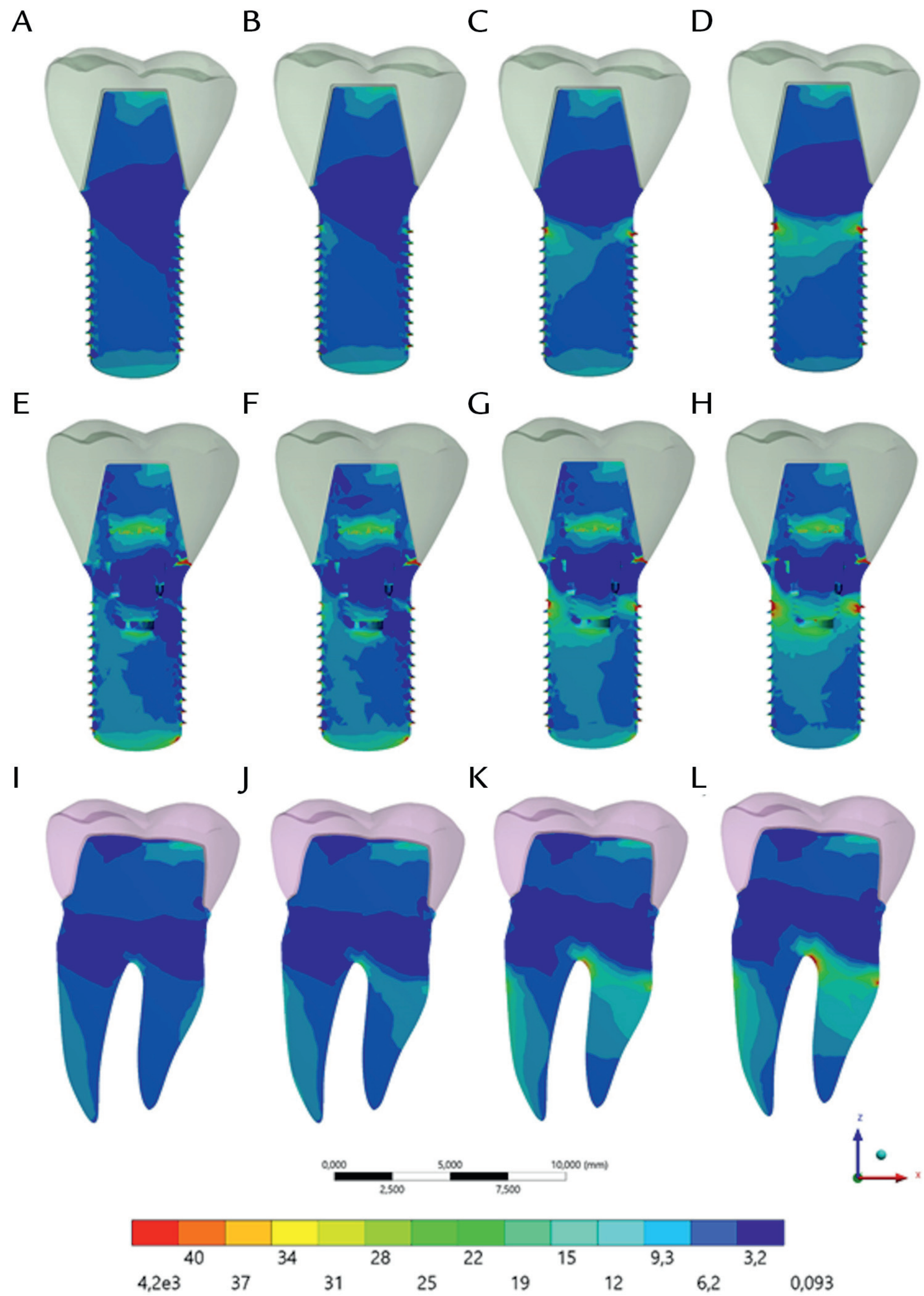

Figure 7. Maximum principal stress (tensile) distribution in implant structure according to different implant designs and bone type. Monotype implant design and bone: A, D1; B, D2; C, D3; D, D4. Two-piece design and bone: E, D1; F, D2; G, D3; H, D4. RAI and bone: I, D1; J, D2; K, D3; L, D4.

the optimal loading distribution when the implant shape follows the nature of the roots.

Even if the RAI is not popular because of difficulties in the fabrication process, the dental community should understand its benefits, including improved esthetics, function, and mechanical behavior.[41] FEA has been applied to compare the stress fields of peri-implant bone around root-analog and screw-shaped conventional zirconia implants.[42] The study revealed that RAIs (with flaps) resulted in better stress distribution in the cortical bone than conventional implants. Their model was created based on a nonspecific single-rooted tooth without a crown. Similar to the present study, the results showed that conventional implants tended to induce some high-stress areas, evidenced by the high values of stress for very small volume fractions. In addition, the authors calculated strain values above 4000 μ-strain for implants with threads;

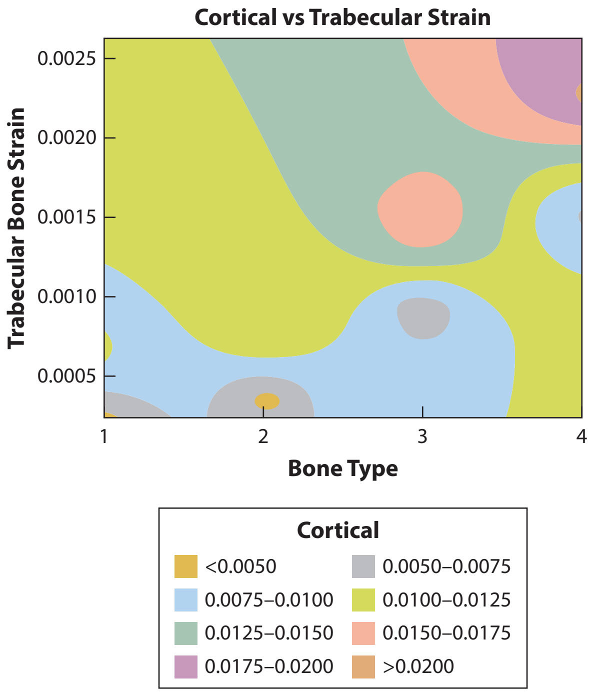

Figure 8. Bone tissue microstrain contour plot exhibiting relationship between fitted response of bone type and bone tissue mechanical response.

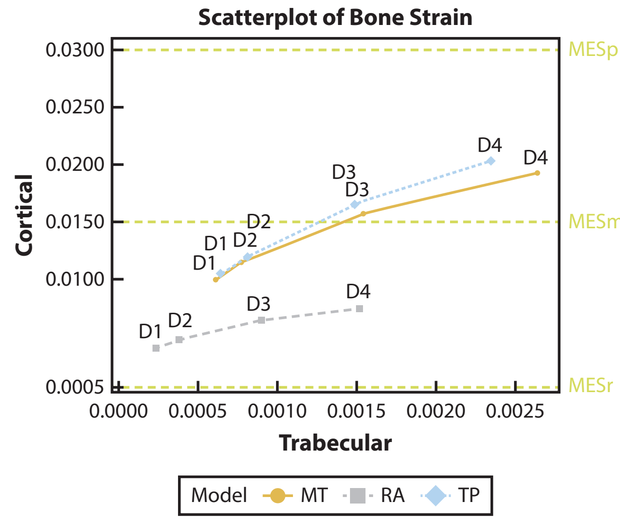

Figure 9. Bone microstrain scatterplot according to bone type (D1, D2, D3, and D4) and monotype (MT), 2-piece (TP), and root-analog (RA) implant designs.

however, they considered that these results were not representative.

When comparing RAIs with a natural tooth, the natural tooth presents the best stress distribution as the periodontal ligament absorbs the loads placed on the tooth during mastication and distributes them to the surrounding bone.[41,42] This favorable effect leads to a more uniform stress distribution in the bone and surrounding structures.[42] Because the missing periodontal ligament cannot be recovered, RAIs can be assumed to behave almost like an ankylosed tooth, without the benefits of the periodontal ligament but keeping the bone shape as it was before the extraction and improving the load dissipation to the bone.

A follow-up of 31 RAIs reported a survival rate of 94.4% at 18.9 months after the surgery.[43] The individual sensation, at rest or in function, was rated as 89.1%, and the esthetic perception was evaluated as 91.6%. According to the authors, the influence of implant and abutment portion location on marginal bone remodeling and a more reliable evaluation of the 3D resorption processes would be of interest.[43] The present study showed the 3D mechanical response of a posterior RAI, suggesting that, in the future, a mechanical analysis could be performed before the surgical stage to elucidate whether an RAI would benefit each patient. Supporting the use of a mechanical analysis, previous in vitro studies concluded that stress is a promotional effect of mechanical loading on osteoblast proliferation,[44] as well as enhancing osteoclast precursor cells.[45] This means that the load-induced strain is closely related to alveolar resorption and formation in cortical bone[46] and alveolar bone tissues[47] as an effect of the mechanotransduction phenomenon. Therefore, the bone cell activity related to alveolar resorption and formation is dependent on the local strain associated with implant loading[48] and could be benefited by the theoretical analysis of stress and strain. Limitations of 3D FEA included that all the factors in the oral medium were not considered, that all crowns were modeled with an ideal bond strength and adaptation, and that this study simulated a molar tooth with specific shape and anatomy. Further studies should elucidate the effect of different anatomies, bone maturation stages, parafunctional loading, fatigue effect, and alternative biomaterials.

CONCLUSIONS

Based on the findings of this 3D FEA study, the following conclusion was drawn:

1. The biomechanical behavior of the zirconia root-analog implant (RAI) for molar rehabilitation suggests that it is more promising for masticatory load dissipation than conventional screw-shaped implants.

REFERENCES

1. Walker A. Diet and teeth. Dietary hypotheses and human evolution. *Philos Trans R Soc Lond B Biol Sci*. 1981;292:57–64.
2. Smith TM. Teeth and human life-history evolution. *Annu Rev Anthropol*. 2013;42:191–208.
3. Lang NP. Oral implants: the paradigm shift in restorative dentistry. *J Dent Res*. 2019;98:1287–1293.
4. Jemt T, Eriksson J. Implant failures before and after peri-implantitis surgery: a retrospective study on 207 consecutively treated patients. *Clin Implant Dent Relat Res*. 2020;22:567–573.

5. Derks J, Tomasi C. Peri-implant health and disease. A systematic review of current epidemiology. *J Clin Periodontol*. 2015;42:S158–S171.
6. González-Serrano J, Molinero-Mourelle P, Pardal-Peláez B, Sáez-Alcaide LM, Ortega R, López-Quiles J. Influence of short implants geometry on primary stability. *Med Oral Patol Oral Cir Bucal*. 2018;23:e602–e607.
7. Agustín-Panadero R, León-Martínez R, Labaig-Rueda C, Faus-López J, Solá-Ruíz MF. Influence of implant-prosthetic connection on peri-implant bone loss: a prospective clinical trial with 2-year follow-up. *Int J Oral Maxillofac Implants*. 2019;34:963–968.
8. O'Sullivan D, Sennerby L, Meredith N. Influence of implant taper on the primary and secondary stability of osseointegrated titanium implants. *Clin Oral Implants Res*. 2004;15:474–480.
9. Abuhussein H, Pagni G, Rebaudi A, Wang HL. The effect of thread pattern upon implant osseointegration. *Clin Oral Implants Res*. 2010;21:129–136.
10. Silveira MPM, Campaner LM, Bottino MA, Nishioka RS, Borges ALS, Tribst JPM. Influence of the dental implant number and load direction on stress distribution in a 3-unit implant-supported fixed dental prosthesis. *Dent Med Probl*. 2021;58:69–74.
11. Van Oers RF, Feilzer AJ. Abutment-to-fixture load transfer and peri-implant bone stress. *Am J Dent*. 2015;28:247–250.
12. Fu JH, Wang HL. Breaking the wave of peri-implantitis. *Periodontology*. 2000;84:145–160.
13. Brånemark PI, Adell R, Breine U, Hansson BO, Lindström J, Ohlsson A. Intra-osseous anchorage of dental prostheses. I. Experimental studies. *Scand J Plast Reconstr Surg*. 1969;3:81–100.
14. Sadowsky SJ. Occlusal overload with dental implants: a review. *Int J Implant Dent*. 2019;5:29.
15. Onclin P, Slot W, Vissink A, Raghoebar GM, Meijer HJA. Incidence of peri-implant mucositis and peri-implantitis in patients with a maxillary overdenture: A sub-analysis of two prospective studies with a 10-year follow-up period. *Clin Implant Dent Relat Res*. 2022;24:188–195.
16. Kesar N, Weigl P, Nentwig GH, Krebs M. Prevalence and risk of peri-implant diseases based on the type of prosthetic restoration: A retrospective study after 17 to 23 years. *J Prosthet Dent*. 8 January 2022. https://doi.org/10.1016/j.prosdent.2021.11.030 [Epub ahead of print.].
17. Frost HM. Wolff's law and bone's structural adaptations to mechanical usage: an overview for clinicians. *Angle Orthod*. 1994;64:175–188.
18. Misch Carl E. *Dental implant prosthetics-E-book*. 1st ed. St. Louis: Elsevier Health Sciences; 2004:130–141.
19. Regish KM, Sharma D, Prithviraj DR. An overview of immediate root analogue zirconia implants. *J Oral Implantol*. 2013;39:225–233.
20. Figliuzzi MM, Aiello D, Rengo C, Parentela L, Mangano C. 10-year evaluation of the first root analogue implant on humans, made using a CT scan, CAD/CAM and DMLS. *Biomimetics (Basel)*. 2022;7:32.
21. Liu Y, Sing SL, Lim RXE, Yeong WY, Goh BT. Preliminary investigation on the geometric accuracy of 3D printed dental implant using a monkey maxilla incisor model. *Int J Bioprint*. 2022;8:476.
22. de Matos JDM, Lopes GDRS, Nakano LJN, et al. Biomechanical evaluation of 3-unit fixed partial dentures on monotype and two-piece zirconia dental implants. *Comput Methods Biomech Biomed Engin*. 2022;25:239–246.
23. Martinez H, Davarpanah M, Missika P, Celletti R, Lazzara R. Optimal implant stabilization in low density bone. *Clin Oral Implants Res*. 2001;12:423–432.
24. Taylor AR. Scialom (aiguilles) needle implants. *Dent News (Lond)*. 1968;5:2.
25. Pasqualini U, Pasqualini ME. *Treatise of Implant Dentistry: The Italian Tribute to Modern Implantology*. Carimate, IT: Ariesdue; 2009:1–11.
26. Vernole B, Geyer A, Pasqualini U. Impianti endoossei a lama. La preparazione del solco chirurgico con la ruota dentata di geyer. tecnica personale [Endosseous blade implantation. Preparation of the surgical sulcus with Geyer's cogwheel. Author's personal method]. *Minerva Stomatol*. 1973;22:266–268.
27. Tada S, Stegaroiu R, Kitamura E, Miyakawa O, Kusakari H. Influence of implant design and bone quality on stress/strain distribution in bone around implants: a 3-dimensional finite element analysis. *Int J Oral Maxillofac Implants*. 2003;18:357–368.
28. Meng HW, Chien EY, Chien HH. Dental implant bioactive surface modifications and their effects on osseointegration: a review. *Biomark Res*. 2016;4:24.
29. Moin DA, Hassan B, Mercelis P, Wismeijer D. Designing a novel dental root analogue implant using cone beam computed tomography and CAD/CAM technology. *Clin Oral Implants Res*. 2013;24:25–27.
30. Liu M, Wang Y, Zhang S, Wei Q, Li X. Success factors of additive manufactured root analogue implants. *ACS Biomater Sci Eng*. 2022;8:360–378.
31. Lundgren D, Rylander H, Andersson M, Johansson C, Albrektsson T. Healing-in of root analogue titanium implants placed in extraction sockets. An experimental study in the beagle dog. *Clin Oral Implants Res*. 1992;3:136–143.
32. Trindade FZ, Valandro LF, de Jager N, Bottino MA, Kleverlaan CJ. Elastic properties of lithium disilicate versus feldspathic inlays: effect on the bonding by 3D finite element analysis. *J Prosthodont*. 2018;27:741–747.
33. Campaner LM, Ribeiro AO, Tribst JPM, et al. Loading stress distribution in posterior teeth restored by different core materials under fixed zirconia partial denture: A 3D-FEA study. *Am J Dent*. 2021;34:157–162.
34. Kumar N, Ramakrishnan SA, Lopez KG, et al. Can polyether ether ketone dethrone titanium as the choice implant material for metastatic spine tumor surgery? *World Neurosurg*. 2021;148:94–109.
35. Schweiger J, Edelhoff D, Güth JF. 3D printing in digital prosthetic dentistry: an overview of recent developments in additive manufacturing. *J Clin Med*. 2021;10:2010.
36. Dantas T, Madeira S, Gasik M, Vaz P, Silva F. Customized root-analogue implants: a review on outcomes from clinical trials and case reports. *Materials (Basel)*. 2021;14:2296.
37. Lin C, Hu H, Zhu J, Rong Q, Tang Z. Influence of different diameter reductions in the labial neck region on the stress distribution around custom-made root-analogue implants. *Eur J Oral Sci*. 2022;130, e12833.
38. de Graaf NPJ, Feilzer AJ, Kleverlaan CJ, Bontkes H, Gibbs S, Rustemeyer T. A retrospective study on titanium sensitivity: patch test materials and manifestations. *Contact Dermatitis*. 2018;79:85–90.
39. Gibbs S, Kosten I, Veldhuizen R, et al. Assessment of metal sensitizer potency with the reconstructed human epidermis IL-18 assay. *Toxicology*. 2018;393:62–72.
40. Saeidi Pour R, Freitas Rafael C, Engler MLPD, et al. Historical development of root analogue implants: a review of published papers. *Br J Oral Maxillofac Surg*. 2019;57:496–504.
41. Burr DB, Allen MR. *In Basic and applied bone biology*. Academic Press; 2014:225–242.
42. Dantas TA, Carneiro Neto JP, Alves JL, Vaz PCS, Silva FS. In silico evaluation of the stress fields on the cortical bone surrounding dental implants: comparing root-analogue and screwed implants. *J Mech Behav Biomed Mater*. 2020;104:103667.
43. Böse MWH, Hildebrand D, Beuer F, et al. Clinical outcomes of root-analogue implants restored with single crowns or fixed dental prostheses: a retrospective case series. *J Clin Med*. 2020;9:2346.
44. Yan YX, Gong YW, Guo Y, et al. Mechanical strain regulates osteoblast proliferation through integrin-mediated ERK activation. *PLoS one*. 2012;7:e35709.
45. Kadow-Romacker A, Duda GN, Bormann N, Schmidmaier G, Wildemann B. Slight changes in the mechanical stimulation affects osteoblast- and osteoclast-like cells in co-culture. *Transfus Med Hemother*. 2013;40:441–447.
46. Chow DH, Leung KS, Qin L, Leung AH, Cheung WH. Low-magnitude high-frequency vibration (LMHFV) enhances bone remodeling in osteoporotic rat femoral fracture healing. *J Orthop Res*. 2011;29:746–752.
47. Xu Q, Yuan X, Zhang X, et al. Mechanoadaptive responses in the periodontium are coordinated by wnt. *J Dent Res*. 2019;98:689–697.
48. Okawara H, Arai Y, Matsuno H, et al. Effect of load-induced local mechanical strain on peri-implant bone cell activity related to bone resorption and formation in mice: an analysis of histology and strain distributions. *J Mech Behav Biomed Mater*. 2021;116:104370.

Corresponding author:
Dr João Paulo Mendes Tribst
Academic Centre for Dentistry Amsterdam (ACTA)
Universiteit van Amsterdam and Vrije Universiteit
Gustav Mahlerlaan 3004, 1081 LA Amsterdam. Noord-Holland
THE NETHERLANDS.
Email: j.p.mendes.tribst@acta.nl

https://doi.org/10.1016/j.prosdent.2022.10.005